Materials Research Express

PAPER

Tunable electronic properties of InSe by biaxial strain: from bulk to single-layer

To cite this article: Khang D Pham *et al* 2019 *Mater. Res. Express* **6** 115002

View the article online for updates and enhancements.

IOP ebooks™

Bringing you innovative digital publishing with leading voices to create your essential collection of books in STEM research.

Start exploring the collection - download the first chapter of every title for free.

This content was downloaded from IP address 129.100.58.76 on 24/10/2019 at 11:21

IOP Publishing Mater. Res. Express 6 (2019) 115002 https://doi.org/10.1088/2053-1591/ab43ea

Materials Research Express

RECEIVED
5 May 2019

REVISED
18 July 2019

ACCEPTED FOR PUBLICATION
12 September 2019

PUBLISHED
25 September 2019

PAPER

Tunable electronic properties of InSe by biaxial strain: from bulk to single-layer

Khang D Pham[1,2], **Vo T T Vi**[3,4], **Doan V Thuan**[5], **Le T T Phuong**[3], **Le T Hoa**[3], **Nguyen V Hieu**[6,11], **Chuong V Nguyen**[7], **Huynh V Phuc**[8], **Hamad R Jappor**[9], **Nguyen Q Cuong**[3], **Bui D Hoi**[3] and **Nguyen N Hieu**[10,11]

[1] Laboratory of Applied Physics, Advanced Institute of Materials Science, Ton Duc Thang University, Ho Chi Minh City, Viet Nam
[2] Faculty of Applied Sciences, Ton Duc Thang University, Ho Chi Minh City, Viet Nam
[3] Department of Physics, University of Education, Hue University, Hue, Viet Nam
[4] Department of Fundamental Sciences, University of Medicine and Pharmacy, Hue University, Hue, Viet Nam
[5] NTT Hi-Tech Institute, Nguyen Tat Thanh University, Ho Chi Minh City, Viet Nam
[6] Department of Physics, University of Education, The University of Da Nang, Da Nang, Viet Nam
[7] Department of Materials Science and Engineering, Le Quy Don Technical University, Ha Noi, Viet Nam
[8] Division of Theoretical Physics, Dong Thap University, Dong Thap, Viet Nam
[9] Department of Physics, College of Education for Pure Sciences, University of Babylon, Hilla, Iraq
[10] Institute of Research and Development, Duy Tan University, Da Nang 550000, Viet Nam
[11] Author to whom any correspondence should be addressed.

E-mail: phamdinhkhang@tdtu.edu.vn, nvhieu@ued.udn.vn and hieunn@duytan.edu.vn

Keywords: single-layer InSe, strain engineering, electronic properties, first-principles calculations

Abstract

In the present work, we consider the electronic properties of bulk and single-layer InSe using the density functional theory. Our calculations show that at the equilibrium state, the single-layer InSe is a semiconductor with an indirect energy bandgap of 1.382 1 eV, nearly twice the bandgap of bulk InSe. Focusing on the effect of biaxial strain ε_b on electronic properties of single-layer InSe, our calculated results indicate that tensile biaxial strain changes slightly the valence subbands near Fermi level, while the band structure of the single-layer InSe depends tightly on the compressive biaxial strain. Also, the energy gap of the single-layer InSe depends almost linearly on the ε_b. However, the energy gap tends to increase slowly when the large compressive biaxial strain is applied. We believe that the control of the energy gap of the single-layer InSe by strain engineering can be useful in its application in nanoelectromechanical systems and nanoelectronic devices.

1. Introduction

The rise of graphene [1] has been a driving force for scientists studying two-dimensional materials for more than a decade. After graphene, many theoretical studies and experimental measurements have been focused on a layered two-dimensional (2D) materials, such as phosphorene [2], silicene [3], stanene [4], and germanene [5]. At the same time, many new materials have been discovered and joined to the 2D family, highlighting single-layers of dichalcogenides [6–9] and monochalcogenides [10–12] or the 2D-based van der Waals heterostructures [13–15] with many outstanding physical properties. Interestingly, the monochalcogenides usually have a wide natural bandgap. This feature has overcome the biggest disadvantage of graphene which has the zero-bandgap that has caused many difficulties in its application to nanoelectronic technologies.

Recently, several single-layers of group III-V binary compounds have been successfully synthesized [16–18]. Among these, the single-layer InSe is of great interest to scientists because of its stable structure [11] and potential for applications in opto-electronics and nano-electronic devices [19]. It exhibits excellent mechanical flexibility with the uniaxial strain threshold of up to 25% and thermodynamically stable at room temperature [20]. Also, via investigations of the strain-stress relations and Young's modulus, one also indicated that the strain threshold of the single-layer InSe is very close to that of other 2D materials such as single-layer SnS which has an outstanding mechanical stability with the threshold of compressive strain is up to −20% [21] or phosphorene

© 2019 IOP Publishing Ltd

can stable under a large range of the applied strain from −16% to 20% [22]. At liquid-helium temperature, carrier mobilities of the few-layer InSe were found up to 10^4 cm^2 V^{-1} s^{-1} [23]. Besides, the single-layer InSe is predicted to be a promising candidate for applications in optoelectronics because of its tunable optical properties due to strong charge transfer and adsorption-induced in-gap states [24]. Moreover, the single-layer InSe has great potential in gas sensor applications since it has recognizable properties when interacting with different gas molecules [24, 25].

The single-layer InSe is one of the members of 2D layered materials family formed from the metal atoms In and chalcogen atoms Se arranged in the honeycomb lattice via four covalently bonds Se–In–In–Se. Electronic and transport properties of the single-layer InSe have been investigated by various approaches [11, 26, 27]. Demirci and his group have shown that the single-layer InSe at equilibrium is a semiconductor with an indirect energy gap of 1.37 eV [11]. However, the computed value of bandgap depends strongly on the selected exchange–correlation energy functionals. Effects of strains [20, 28, 29] and electric field [30] on electronic properties of the single-layer InSe have also been investigated by first-principles calculations. Besides, calculations on the electronic properties of few-layer InSe or InSe-based van der Waals (vdW) heterostructures have been recently reported [31–35]. They indicated that the InSe-based vdW heterostructures are an excellent candidate for applications in light emission devices and high-efficiency solar cell [36]. Besides, Fan and co-workers also demonstrated that the InSe can be a perfect substrate for the growth of germanene and silicene for nanoelectronic devices [37].

Although the single-layer InSe has many outstanding physical and chemical properties. However, there are still obstacles in applying the single-layer InSe into the real nanoelectronic device. Therefore, continuing basic research on electronic properties of single-layer InSe, especially in the presence of a mechanical strain or an external electric field, is still very necessary to get more information on how to use it in technologies. In this work, we systematically consider the effect of the biaxial strain ε_b on the electronic properties of the single-layer InSe using density functional theory (DFT). We also investigate the electronic properties of the bulk InSe to compare with the single-layer case. Besides, the dependence of the energy gap of the single-layer InSe on the strain is particularly noted in the present work.

2. Model and computational details

In the present study, we calculate the structural and electronic properties of both bulk and single-layer InSe by density functional theory (DFT), implemented by the Quantum ESPRESSO package [38] with the generalized gradient approximations (GGA). The accurate projector augmented-wave (PAW) pseudopotentials [39, 40] and the Perdew–Burke–Ernzerhof (PBE) exchange–correlation energy functional [41, 42] have been used in the calculations. In order to describe a long-range weak vdW interactions occurring in layered bulk InSe, a semi-empirical DFT-D2 method [43] was adopted. For sampling the first Brillouin zone, in this work we use the $(15 \times 15 \times 1)$ k-mesh Monkhorst–Packgrid. The kinetic energy cut-off for plane-wave basis was set as 37 Ry. The structures of the InSe are fully relaxed with convergence criteria for the force acting on each atom less than 10^{-6} Ry/cell. To consider the effect of a biaxial strain ε_b on the electronic properties of the single-layer InSe, we define the biaxial strain ε_b via the lattice constant. The biaxial strain ε_b is applied to the InSe single-layer by varying its lattice constant as $\varepsilon_b = (\delta - \delta_0)/\delta_0$, where δ_0 and δ are the lattice constants of the single-layer InSe at equilibrium and under strain, respectively. In the present work, all structural geometries, including unstrained and strained structures, were relaxed to obtain the equilibrium atomic positions in its unit cell. After that, we calculate the electronic band structures of the unstrained and strained systems. We focus on the electronic properties of the single-layer InSe under the biaxial strain ε_b ranging from −10% to 10%. The minus sign represents the compression case.

3. Results and discussion

Firstly, we focus on the structural properties and geometric features of InSe. Figure 1 illustrates an atomic structure of the InSe. There are four atom layers along the z-axis with the ordering of Se–In–In–Se in each single-layer InSe as shown in figure 1(b). In the multilayers InSe, the van der Waals forces will keep the individual single-layers tightly held together. At the equilibrium, the calculated lattice parameters of the bulk InSe are $a = b = 3.94$ Å and $c = 16.85$ Å. The thickness of an individual layer in bulk InSe (Se–Se distance) is equal to 5.46 Å. This result is in good agreement with an available data [44]. The computed results for the lattice parameters are also listed in table 1.

Our DFT calculations indicate that the bulk InSe at equilibrium is an indirect semiconductor and its band gap is 0.75 eV. However, in the bulk InSe, the difference between this indirect bandgap (0.75 eV) and a direct bandgap (0.76 eV) opening at the S point is extremely small. In previous DFT work, Sun and co-workers showed

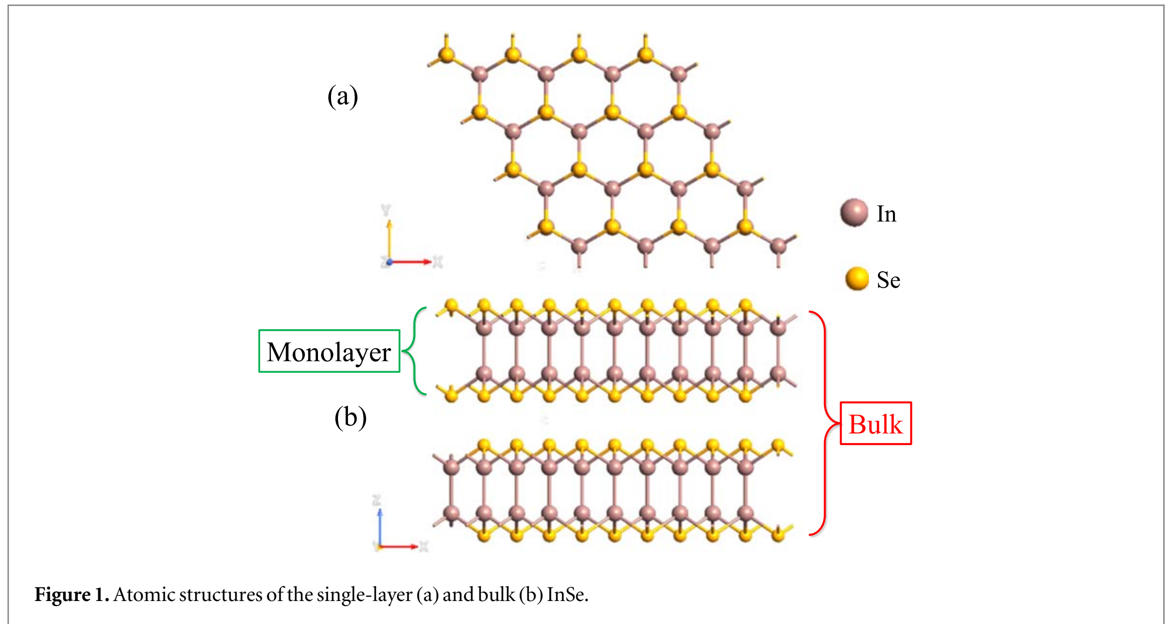

Figure 1. Atomic structures of the single-layer (a) and bulk (b) InSe.

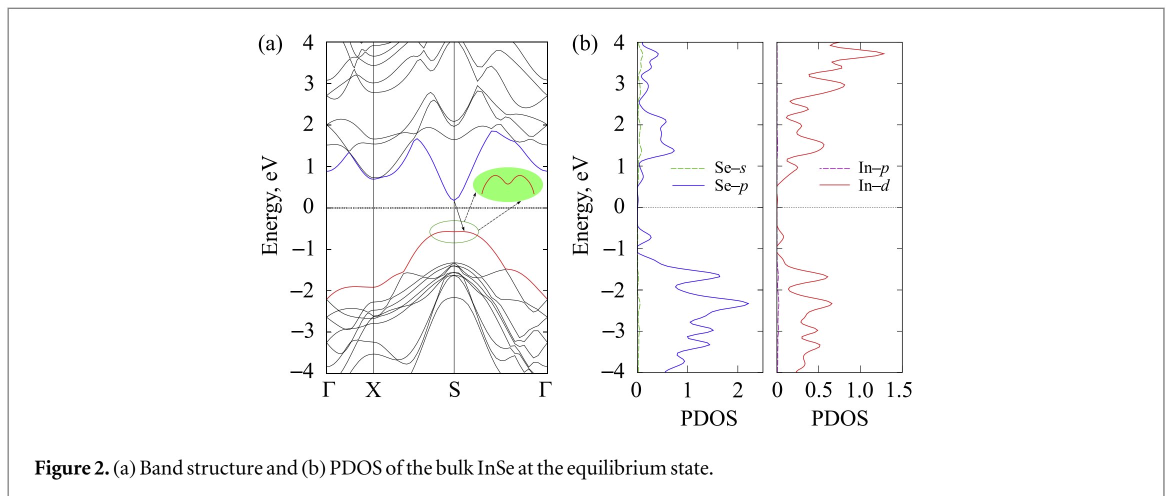

Figure 2. (a) Band structure and (b) PDOS of the bulk InSe at the equilibrium state.

Table 1. Calculated lattice constants (a and c), bond lengths (d_{In-Se} and d_{In-In}), Se–Se distance (d_{Se-Se}, thickness of an individual layer), total energy (E_{tot}), and bandgap (E_g) of the bulk and single-layer InSe.

	$a = b$, Å	c, Å	d_{In-Se}, Å	d_{In-In}, Å	d_{Se-Se}, Å	E_{tot}, eV	E_g, eV
Bulk	3.94	16.85	2.64	2.77	5.46	−32 665.15	0.75
single-layer	3.89	—	2.58	2.81	5.35	−16 332.28	1.38

that five-layer InSe has an indirect bandgap of 0.68 eV [45]. Besides, one showed the bandgap of the bulk InSe being 0.41 eV by DFT calculations [26]. Meanwhile, experimental measurements for the bandgap of the bulk InSe are much larger than that by DFT calculations being 1.25 eV [18] and 1.54 [46, 47] at the room temperature [18] or 1.40 eV at the low temperature [48]. In the framework of DFT, underestimation in bandgap calculations of the traditional DFT methods, such as Local-density approximations (LDA) and GGA approximation, is the cause of the discrepancies in the calculated bandgap results. Also, the bandgap problem can be fixed by using GW approximation [49]. However, this trend is not the generalization and depends strongly on the considered materials. In figure 2, we show the energy band structure and partial density of states (PDOS) of the bulk InSe at the equilibrium state. It indicates that while the conduction band minimum (CBM) locates at the S-point, the valence band maximum (VBM) locates on the SΓ or XS-path (the valence band has two maxima, which are symmetric with each other passing through the line passing through S point). From figure 2(b) we can see that, at the equilibrium state, both top of the valence band and bottom of the conduction band of the bulk InSe are

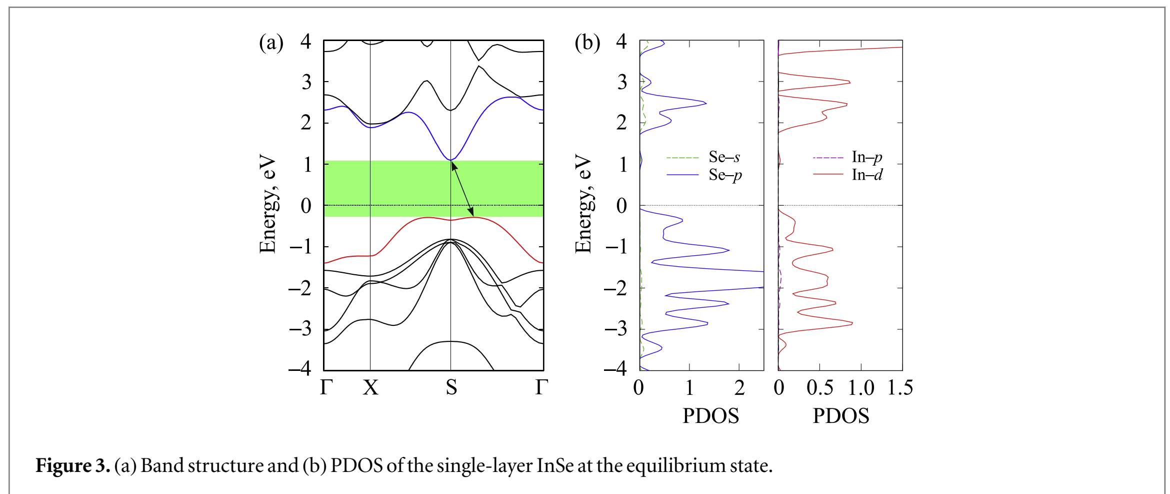

Figure 3. (a) Band structure and (b) PDOS of the single-layer InSe at the equilibrium state.

mainly donated from the In-*d* orbitals. The In-*d* orbitals, however, donate mainly to the bottom of the conduction band while the contribution of the Se-*p* orbitals is dominant for the top of the valence band of the bulk InSe.

Recently, single-layer InSe has successfully been synthesized by various experimental methods [50]. The atomic structure of single-layer InSe is built based on experimental pattern and it is similar to the structure of the single-layers GaS and GaSe, which have also been successfully synthesized ealier [51, 52]. Geometrically, the single-layer InSe belongs to the D_{3h} space group [11, 26]. The calculated structural parameters of the single-layer InSe show that the lattice parameters are $a = b = 3.89$ Å at the equilibrium state. The single-layer thickness (Se–Se distance) is 5.35 Å. Our calculated results are good in agreement with the previous DFT caluclations [11, 53]. Electronic band structure and PDOS of the single-layer InSe at equilibrium are shown in figure 3. We can see that the single-layer InSe at equilibrium is an indirect semiconductor with an energy gap of $E_g = 1.38$ eV. Our calculated result is a good agreement with the previous DFT calculations [11, 20]. Table 1 indicates that, at the equilibrium state, the E_g of the single-layer InSe is 1.38 eV, nearly twice the energy gap of bulk InSe. However, it is easy to see that the position of the VBM and CBM in the single-layer InSe is the same as in the bulk materials. The CBM is at S-point and the VBM is close to the S-point. To better understand the contribution of the orbital atoms to the band structure of the single-layer InSe, we provide the PDOS of the InSe single-layer as shown in figure 3(b). Similar to the bulk case, the contribution from orbitals of the In-*d* and Se-*p* to the electronic states near the Fermi level in the single-layer InSe is remarkable. In the valence band, the contribution of the Se-*p* orbitals to the total density of states is greater than that of In-*d*. Meanwhile, the contribution from the In-*d* orbitals to the density of states is slightly larger than that from Se-*p* orbitals.

We next consider the influence of a biaxial strain ε_b on electronic properties of the single-layer InSe. From calculations of the phonon spectrum, the previous work showed that the structure of the single-layer InSe is dynamically stable because there are no soft phonons in its phonon dispersion curves [11].

In figure 4 we show the calculated result for the total energy of the single-layer InSe when the ε_b is applied. The minimum total energy is at the equilibrium state $\varepsilon_b = 0$ being $-16\,332.28$ eV and the tensile strain increases the total energy faster than the compressive case in the strain range from -10% to 10%. Band structure of the single-layer InSe under biaxial strain with various elongations ε_b is shown in figure 5. We can see that the VBM is almost unchanged under the impact of the tensile biaxial strain ($\varepsilon_b > 0$) and, therefore, the influence of the tensile biaxial strain on bandgap is due to the change of the CBM. Focusing on the subbands of the valence band near the Fermi level at the equilibrium (see figure 5(c)), we can see that the VBM and the maximum energy value of the valence band at the S point are energetically very close. They look like degenerate points. We expect that the position of the VBM of the single-layer InSe will change as is affected by external factors such as strain, which can cause the indirect–direct transition in the single-layer when the ε_b is applied. However, our calculated results demonstrate that there is no indirect–direct transition in InSe in the presence of the ε_b. Interestingly, the strain ε_b can cause the VBM to move to the S point but, at the same time, it also causes the CBM to move to the Γ point as shown in figure 5(a). The PDOS of the single-layer InSe under the ε_b is also presented in figure 6. Effect of the ε_b on the bandgap of the single-layer InSe is shown in figure 7. In the biaxial strain range from -10% to 10%, we can see that the bandgap of the single-layer InSe depends almost linearly on the ε_b. However, the bandgap tends to increase slowly when the large compressive biaxial strain is applied. The shape of the bandgap dependence on the biaxial strain ε_b is consistent with the calculations in the previous study [20, 28]. The control

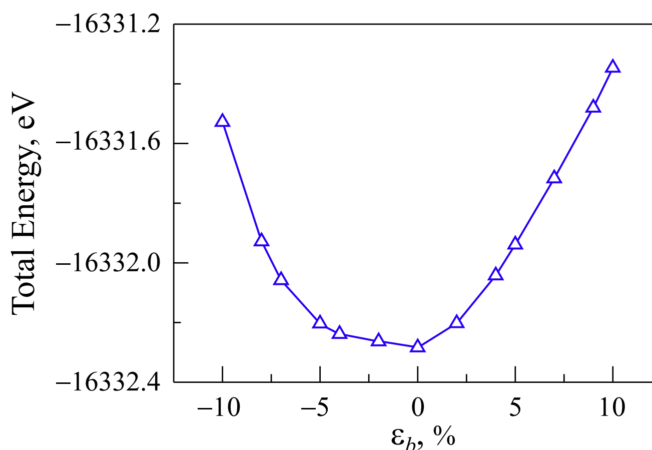

Figure 4. Total energy of the single-layer InSe under the biaxial strain ε_b.

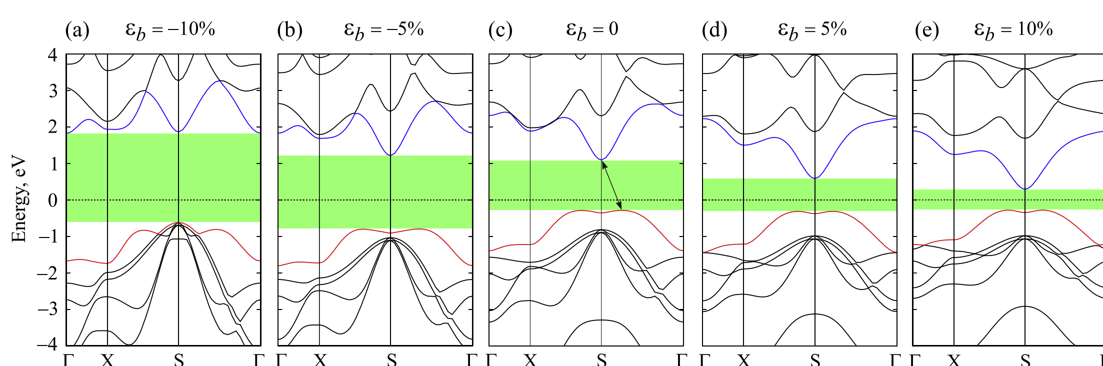

Figure 5. Band structure of single-layer under biaxial strain at (a) $\varepsilon_b = -10\%$, (b) $\varepsilon_b = -5\%$, (c) $\varepsilon_b = 0\%$ (at equilibrium), (d) $\varepsilon_b = 5\%$, and (e) $\varepsilon_b = 10\%$.

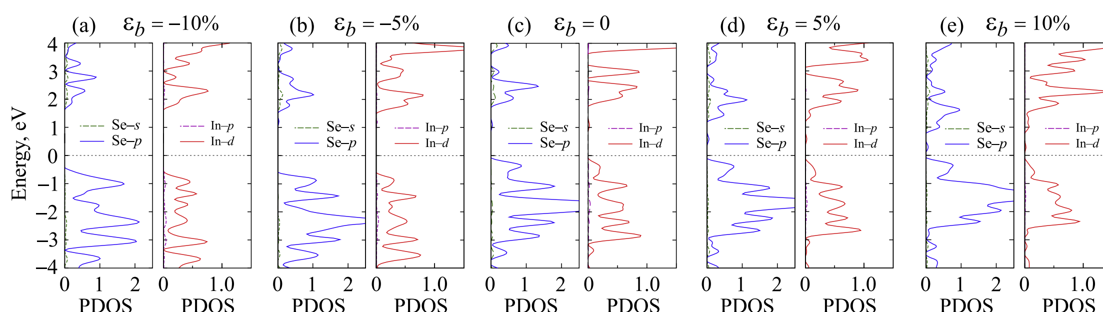

Figure 6. Partial density of states (PDOS) of the single-layer InSe under the biaxial strain at (a) $\varepsilon_b = -10\%$, (b) $\varepsilon_b = -5\%$, (c) $\varepsilon_b = 0\%$ (at equilibrium), (d) $\varepsilon_b = 5\%$, and (e) $\varepsilon_b = 10\%$.

of energy bandgap by strain is one of the most important techniques in the application of semiconductor materials, especially the 2D materials which are sensitive to the strain, to nanoelectronic technologies.

4. Conclusion

In conclusion, we have systematically considered the effect of the biaxial strain on the structural and electronic properties of the single-layer InSe by using the DFT calculations. Our calculated results show that, at the equilibrium state, the single-layer is the semiconductor with the indirect bandgap of 1.38 eV, which is greater

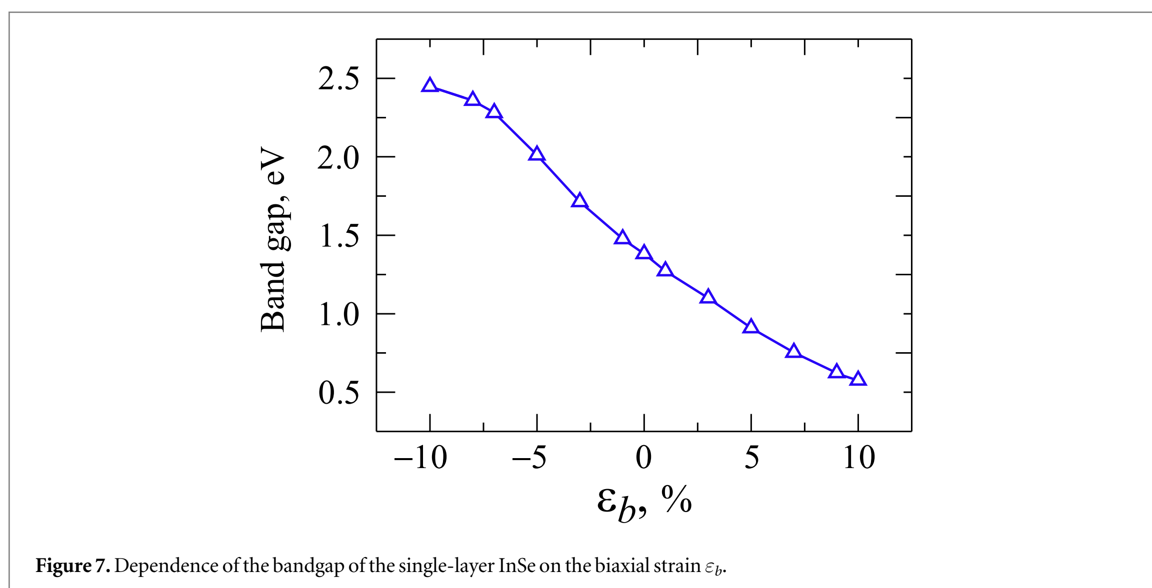

Figure 7. Dependence of the bandgap of the single-layer InSe on the biaxial strain ε_b.

than that of the bulk InSe nearly twice (0.75 eV). In the presence of the biaxial strain ε_b, the bandgap of the single-layer InSe decreases almost linearly with the ε_b changing from −10% to 10%. In the case of $\varepsilon_b < 0$, the strain is not only a cause of increasing the bandgap but also of a significant change in the electronic energy band structure, namely position of the CBM and VBM, of the single-layer InSe. We believe that the ability to control the bandgap of the single-layer InSe by strain can provide useful ways for its applications in nanoelectronic devices and nanoelectromechanical systems.

Acknowledgments

This work is funded by the Vietnam Ministry of Education and Training under grant number B2019-DNA-07.

ORCID iDs

Chuong V Nguyen https://orcid.org/0000-0003-4109-7630
Huynh V Phuc https://orcid.org/0000-0001-8063-0923
Hamad R Jappor https://orcid.org/0000-0002-8885-3985
Bui D Hoi https://orcid.org/0000-0002-5174-841X
Nguyen N Hieu https://orcid.org/0000-0001-5721-960X

References

[1] Novoselov K S, Geim A K, Morozov S V, Jiang D, Zhang Y, Dubonos S V, Grigorieva I V and Firsov A A 2004 *Science* **306** 666
[2] Koenig S P, Doganov R A, Schmidt H, Castro Neto A H and Özyilmaz B 2014 *Appl. Phys. Lett.* **104** 103106
[3] Vogt P, De Padova P, Quaresima C, Avila J, Frantzeskakis E, Asensio M C, Resta A, Ealet B and Le Lay G 2012 *Phys. Rev. Lett.* **108** 155501
[4] Zhu F F, Chen W J, Xu Y, Gao C L, Guan D D, Liu C H, Qian D, Zhang S C and Jia J F 2015 *Nat. Mater.* **14** 1020
[5] Liu C C, Feng W and Yao Y 2011 *Phys. Rev. Lett.* **107** 076802
[6] Coleman J N *et al* 2011 *Science* **331** 568
[7] Nguyen C V, Hieu N N, Poklonski N A, Ilyasov V V, Dinh L, Phong T C, Tung L V and Phuc H V 2017 *Phys. Rev.* B **96** 125411
[8] Hieu N N, Ilyasov V V, Vu T V, Poklonski N A, Phuc H V, Phuong L T T, Hoi B D and Nguyen C V 2018 *Superlattices Microstruct.* **115** 10
[9] Nguyen C V, Hieu N N, Muoi D, Duque C A, Feddi E, Nguyen H V, Phuong L T T, Hoi B D and Phuc H V 2018 *J. Appl. Phys.* **123** 034301
[10] Xu L, Yang M, Wang S J and Feng Y P 2017 *Phys. Rev.* B **95** 235434
[11] Demirci S, Avazli N, Durgun E and Cahangirov S 2017 *Phys. Rev.* B **95** 115409
[12] Sahin H, Cahangirov S, Topsakal M, Bekaroglu E, Akturk E, Senger R T and Ciraci S 2009 *Phys. Rev.* B **80** 155453
[13] Phuc H V, Ilyasov V V, Hieu N N, Amin B and Nguyen C V 2018 *J. Alloys Compd.* **750** 765
[14] Hieu N N, Phuc H V, Ilyasov V V, Chien N D, Poklonski N A, Van Hieu N and Nguyen C V 2017 *J. Appl. Phys.* **122** 104301
[15] Phuc H V, Hieu N N, Hoi B D and Nguyen C V 2018 *Phys. Chem. Chem. Phys.* **20** 17899
[16] Lei S, Ge L, Liu Z, Najmaei S, Shi G, You G, Lou J, Vajtai R and Ajayan P M 2013 *Nano Lett.* **13** 2777
[17] Harvey A *et al* 2015 *Chem. Mater.* **27** 3483
[18] Mudd G W *et al* 2013 *Adv. Mater.* **25** 5714
[19] Wang D, Li X B and Sun H B 2017 *Nanoscale* **9** 11619
[20] Hu T, Zhou J and Dong J 2017 *Phys. Chem. Chem. Phys.* **19** 21722

[21] Zhang Y, Shang B, Li L and Lei J 2017 *RSC Adv.* **7** 30327
[22] Hu T and Dong J 2015 *Phys. Rev.* B **92** 064114
[23] Bandurin D A *et al* 2017 *Nat. Nanotechnol.* **12** 223
[24] Cai Y, Zhang G and Zhang Y W 2017 *J. Phys. Chem.* C **121** 10182
[25] Ma D, Ju W, Tang Y and Chen Y 2017 *Appl. Surf. Sci.* **426** 244
[26] Magorrian S J, Zólyomi V and Fal'ko V I 2016 *Phys. Rev.* B **94** 245431
[27] Zhou M, Zhang R, Sun J, Lou W K, Zhang D, Yang W and Chang K 2017 *Phys. Rev.* B **96** 155430
[28] Jalilian J and Safari M 2017 *Phys. Lett.* A **381** 1313
[29] Jin H, Li J, Dai Y and Wei Y 2017 *Phys. Chem. Chem. Phys.* **19** 4855
[30] Wang X P, Li X B, Chen N K, Zhao J H, Chen Q D and Sun H B 2018 *Phys. Chem. Chem. Phys.* **20** 6945
[31] Sun Y, Luo S, Zhao X G, Biswas K, Li S L and Zhang L 2018 *Nanoscale* **10** 7991
[32] Pham K D, Hieu N N, Ilyasov V V, Phuc H V, Hoi B D, Feddi E, Thuan N V and Nguyen C V 2018 *Superlattices Microstruct* **122** 570
[33] Shang J, Pan L, Wang X, Li J and Wei Z 2018 *Semicond. Sci. Technol.* **33** 034002
[34] Zhang Z, Zhang Y, Xie Z, Wei X, Guo T, Fan J, Ni L, Tian Y, Liu J and Duan L 2019 *Phys. Chem. Chem. Phys.* **21** 5627
[35] Pham K D *et al* 2019 *Chem. Phys. Lett.* **716** 155
[36] Shang J, Pan L, Wang X, Li J, Deng H X and Wei Z 2018 *J. Mater. Chem.* C **6** 7201
[37] Fan Y, Liu X, Wang J, Ai H and Zhao M 2018 *Phys. Chem. Chem. Phys.* **20** 11369
[38] Giannozzi P *et al* 2009 *J. Phys.: Condens. Matter* **21** 395502
[39] Blöchl P E 1994 *Phys. Rev.* B **50** 17953
[40] Kresse G and Joubert D 1999 *Phys. Rev.* B **59** 1758
[41] Perdew J P, Burke K and Ernzerhof M 1996 *Phys. Rev. Lett.* **77** 3865
[42] Perdew J P, Burke K and Ernzerhof M 1997 *Phys. Rev. Lett.* **78** 1396
[43] Grimme S 2006 *J. Computat. Chem.* **27** 1787
[44] Wickramaratne D, Zahid F and Lake R K 2015 *J. Appl. Phys.* **118** 075101
[45] Sun C, Xiang H, Xu B, Xia Y, Yin J and Liu Z 2016 *Appl. Phys. Express* **9** 035203
[46] Manjón F J, Segura A, Muñoz-Sanjosé V, Tobías G, Ordejón P and Canadell E 2004 *Phys. Rev.* B **70** 125201
[47] Manjón F J, Errandonea D, Segura A, Muñoz V, Tobías G, Ordejón P and Canadell E 2001 *Phys. Rev.* B **63** 125330
[48] Millot M, Broto J M, George S, González J and Segura A 2010 *Phys. Rev.* B **81** 205211
[49] Debbichi L, Eriksson O and Lebègue S 2015 *J. Phys. Chem. Lett.* **6** 3098
[50] Lauth J *et al* 2016 *Chem. Mater.* **28** 1728
[51] Hu P *et al* 2013 *Nano Lett.* **13** 1649
[52] Late D J, Liu B, Matte H S S R, Rao C N R and Dravid V P 2012 *Adv. Funct. Mater.* **22** 1894
[53] Zólyomi V, Drummond N D and Fal'ko V I 2014 *Phys. Rev.* B **89** 205416